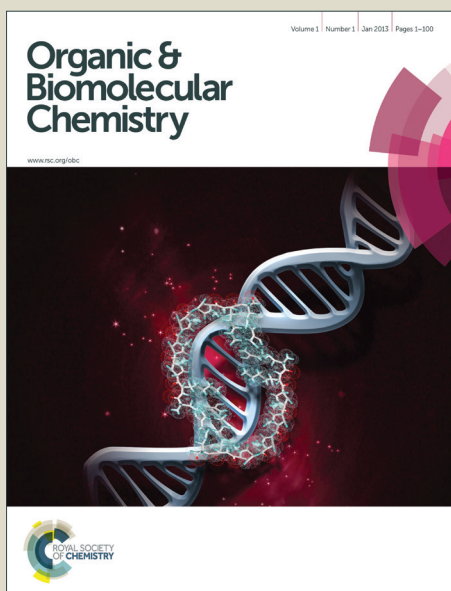


Organic & Biomolecular Chemistry

Accepted Manuscript



This is an *Accepted Manuscript*, which has been through the Royal Society of Chemistry peer review process and has been accepted for publication.

Accepted Manuscripts are published online shortly after acceptance, before technical editing, formatting and proof reading. Using this free service, authors can make their results available to the community, in citable form, before we publish the edited article. We will replace this *Accepted Manuscript* with the edited and formatted *Advance Article* as soon as it is available.

You can find more information about *Accepted Manuscripts* in the [Information for Authors](#).

Please note that technical editing may introduce minor changes to the text and/or graphics, which may alter content. The journal's standard [Terms & Conditions](#) and the [Ethical guidelines](#) still apply. In no event shall the Royal Society of Chemistry be held responsible for any errors or omissions in this *Accepted Manuscript* or any consequences arising from the use of any information it contains.

ARTICLE

Demonstration of a Common Indole-based Aromatic Core in Natural and Synthetic Eumelanins by Solid-State NMR

Subhasish Chatterjee,^{*a} Rafael Prados-Rosales,^b Sindy Tan,^a Boris Itin,^c Arturo Casadevall,^b and Ruth E. Stark^{*a}

Cite this: DOI: 10.1039/x0xx00000x

Received
Accepted

DOI: 10.1039/x0xx00000x

www.rsc.org/

Abstract: Despite the essential functions of melanin pigments in diverse organisms and their roles in inspiring designed nanomaterials for electron transport and drug delivery, the structural frameworks of the natural materials and their biomimetic analogs remain poorly understood. To overcome the investigative challenges posed by these insoluble heterogeneous pigments, we have used L-tyrosine or dopamine enriched with stable ^{13}C and ^{15}N isotopes to label eumelanins metabolically in cell-free and *Cryptococcus neoformans* cell systems and to define their molecular structures and supramolecular architectures. Using high-field two-dimensional solid-state nuclear magnetic resonance (NMR), our study directly evaluates the assumption of structural commonality between synthetic melanin models and the corresponding natural pigments, demonstrating a common indole-based aromatic core in the products from contrasting synthetic protocols for the first time.

Running head: Solid-state NMR of Eumelanins

Keywords: Melanin, *Cryptococcus neoformans*, NMR spectroscopy, Structural Biology, Amorphous materials

ARTICLE

Introduction

Eumelanins, ubiquitous pigments that play protective roles in animals, plants, and fungi,¹ also guide the development of organic nanomaterials with tailored conductive and radical scavenging performance^{2–5} and have applications to soil bioremediation.⁶ Moreover, eumelanins are associated with virulence of fungal pathogens in humans and food crops; these pigments have been implicated in human drug resistance and neuronal degeneration.^{1,7} A related group of bioinspired polydopamine coating materials is emerging as drug delivery vehicles, cell adhesion modulators, and biosensors for drug discovery.⁸ Despite this versatile range of important functions, the insoluble amorphous physical characteristics of eumelanins have impeded efforts to delineate their molecular structures or to critically evaluate the suitability of related synthetic materials as model systems for intact natural pigments with diverse capabilities.⁹

Degradative chemical methods have been employed to identify and quantify the relative proportions of 5,6-Dihydroxyindole (DHI) and 5,6-Dihydroxyindole-2-carboxylic acid (DHICA) as the likely indole-based building blocks of eumelanins.^{9–11} However, diverse linear crosslinked heteropolymers¹² or stacked oligomers^{13,14} can be assembled from just these two monomers in their various tautomeric and redox states to form intractable amorphous melanin pigments; either polymer or oligomer arrangements are expected to produce heterogeneous supramolecular structures that can include chemically similar units.¹⁵ For instance, the currently favoured oligomer models are supported by density functional theory (DFT) but fall short of unique fits to the available physical data or satisfactory accounting for the broad UV-Vis absorbance and humidity-dependent conductivity of the biopolymers.^{15,16} Although synthetic melanins have been implicitly assumed to serve as good models for pigments from natural sources,^{9,11,17} their structural concordance to natural melanins has never been demonstrated directly. Thus, direct molecular and supramolecular information on intact pigments should be of significant value, particularly if obtained for mature melanins produced from defined small-molecule precursors. Such strategies can substantially advance efforts to delineate the formation mechanisms and structural prerequisites of biomaterials that are versatile enough to absorb UV light, bind metals, tailor surfaces for drug resistance, and alter microbial virulence.

Cryptococcus neoformans (CN) is an unusual human pathogenic fungus that forms eumelanins only in the presence of exogenous catecholamine compounds that are oxidatively polymerized by the action of laccase.¹⁸ The requirement of obligatory

catecholamine precursors makes CN a natural platform for generating well-defined eumelanins biosynthetically because it ensures that all melanin products are assembled in the fungal cells from known catecholamine substrates.^{19,20} This requirement also allows us to introduce stable isotope labels that serve as exquisitely sensitive NMR spectroscopic probes of molecular architecture in natural eumelanins.^{21,22} Importantly, the feasibility of making pigments using structurally related catecholamines and different enzyme catalysts under both cell-free conditions and in fungal cells allows us to test how the outcome of melanin formation depends on these controlling factors.

Both solid-state and swelled-solid NMR have been used primarily to deduce the carbon-based functional moieties present in CN eumelanins^{20–22} and related melanin pigments.^{10,23–30} However, nitrogen-based structural information has been sparsely defined for the intact pigments; neither molecular frameworks nor supramolecular organization have been compared systematically for related synthetic and natural eumelanins. Our ability to understand and use eumelanins in bioinspired materials science also remains seriously limited due to the paucity of information about how nitrogenous aromatic compounds build a heterogeneous natural pigment core.

Using isotopically enriched L-tyrosine or dopamine precursors in conjunction with high-field solid-state ¹³C and ¹⁵N NMR of their melanin products, we report the functional groups and, for the first time, the pairwise proximities that define essential features of the carbon-nitrogen molecular framework in intact solid eumelanins. The pigments made by both enzyme-catalyzed chemical polymerization and cell-mediated fungal biosynthesis are shown to possess a common indole-based aromatic core including several magnetically distinct structural frameworks, allowing critical comparison with prior computational and degradative analyses. The current investigation furthers our understanding of the structural arrangements that are prevalent in intact melanins made from indole- and pyrrole-based aromatic building blocks, shedding fresh light on the supramolecular architecture of this important class of enigmatic biomaterials.

Experimental Section

Chemical synthesis of melanins

Chemical reactions were conducted with [U-¹³C, ¹⁵N]-L-tyrosine (Cambridge Isotope Labs, Andover, MA), ¹⁵N-L-tyrosine (Cambridge), L-tyrosine (Sigma Chemical Co., St. Louis, MO),

ARTICLE

L-dopa (Sigma), dopamine (Sigma), and [U-¹³C,¹⁵N]-dopamine precursors (Medical Isotopes, Inc., Pelham, NH) in separate experiments. Other chemicals were purchased from Sigma, unless otherwise stated.

Tyrosinase-mediated oxidative autopolymerization was carried out to form melanin under cell-free conditions essentially as described previously.^{31–33} Briefly, 2.5 mmol of precursor in 100 mL of pH 7.4 sodium phosphate buffer containing 4 mL tyrosinase (667 units/mL) and 1 mL catalase (592 units/mL) was covered with punctured aluminum foil to permit aeration at room temperature (~22 °C) and to avoid extensive oxidation of the developing pigment from peroxide ions generated in the active site of the tyrosinase enzyme. After 72 hours of mechanical stirring, the reaction mixture was acidified to ~pH 1 with 6 M HCl and placed in a boiling water bath for 20 min. The solid pigment was separated by centrifugation at 9000 rpm and 25 °C for 15 min, then washed repeatedly by removing the supernatant after centrifugation and adding distilled water until the pH reached ~7. The precipitate was transferred to a Falcon tube covered with punctured parafilm, frozen using liquid nitrogen, and lyophilized. Upon removal of the sample from the lyophilizer, the sample container was sealed immediately and stored at 4 °C.

The tyrosinase-mediated oxidative process was conducted in the absence of catalase to test the effects of the latter enzyme on generation of melanin pigments under cell-free conditions. Melanins were also produced by autopolymerization of natural abundance L-dopa using published methods^{31–33} as described above but in the absence of the tyrosinase enzyme. The reaction mixtures contained 2.5–5 mmol of L-dopa precursor in 100 mL Tris-HCl (sodium phosphate) buffer at pH 7.4 were covered with punctured aluminum foil to allow for aeration at room temperature (~22 °C). The final products were purified as described above.

CN melanin biosynthesis

Fungal melanins were biosynthesized from the precursors described above using the serotype D 24067 strain of *Cryptococcus neoformans* (American Type Culture Collection 208821) and isolated for biophysical study using chemical protocols that solubilize other cellular components.^{20,34–36} Cells were grown in a 1 mM solution of an obligatory melanin precursor in chemically defined media (29.4 mM KH₂PO₄, 15

mM D-glucose, 13 mM glycine, 10 mM MgSO₄, and 3 μM thiamine at 30 °C) for 10 days at 150 rpm in a rotatory shaker. Either unlabeled or [U-¹³C]-glucose were used in separate experiments. Cell pellets obtained by centrifugation at 2000 rpm were washed with phosphate buffered saline (PBS); the isolated fungal cells were suspended in 1.0 M sorbitol / 0.1 M pH 5.5 sodium citrate solutions and incubated with 10 mg/mL lysing enzymes (from *Trichoderma harzianum*) for 24 h at 30 °C to remove cell walls. After centrifugation at 2000 rpm for 10 mins, the pellet (melanized protoplasts) was washed several times with PBS until the supernatant was nearly clear. To denature proteinaceous components, a 20 mL aliquot of 4.0 M guanidine thiocyanate was added to form a suspension that was incubated for 12 h at room temperature in a rocker (Shaker 35, Labnet, Woodbridge, NJ). The cell debris was collected and washed 2–3 times with ~20 mL PBS and incubated for 4 h at 65 °C in 5 mL of buffer (10 mM Tris-HCl, pH 8.0, 5 mM CaCl₂, 5% SDS) containing 1 mg/mL proteinase K (Boehringer Mannheim, Germany). The recovered cell debris was washed 2–3 times with ~20 mL PBS, then subjected to Folch lipid extraction³⁷ while maintaining the proportions of chloroform, methanol, and saline solution in the final mixture as 8:4:3. After three delipidations, the final product was suspended in 20 mL of 6 M HCl and boiled for 1 h to hydrolyze cellular contaminants associated with melanin. The black particles of interest that survived HCl treatment were dialyzed against distilled water for 14 d with daily water changes. The resulting melanin particles ('ghosts') were lyophilized for further biophysical analysis.

Solid-State NMR

Either of two instruments was used for ¹³C and ¹⁵N solid-state cross polarization – magic-angle spinning (CPMAS) NMR measurements: a Varian (Agilent) VNMR-S NMR spectrometer operating at a ¹H frequency of 600 MHz with a 1.6-mm HXY fastMAS probe equipped to hold 2–6 mg of powdered samples and spinning typically at 15 kHz (±20 Hz) (Agilent Technologies, Santa Clara, CA); or a Bruker Avance II spectrometer operating at a ¹H frequency of 750 MHz with 3.2 mm HCN or 3.2 mm E-free HCN probes containing 6–16 mg of powdered samples and spinning typically at 10–20 kHz (±5 Hz) (Bruker BioSpin Corp., Billerica, MA). All data were collected at spectrometer-set temperatures of 25 °C. Typical 90° pulse lengths for ¹H were ~2.5 μs for the Bruker HCN probe and ~3 μs for the E-free HCN probe; ¹³C and ¹⁵N 90° pulse lengths were ~5 μs and ~6 μs, respectively, for the 3.2 mm HCN probes. For the 1.6-mm

ARTICLE

Varian HXY fastMAS probe, the typical ^1H 90° pulse length was ~ 1.2 μs ; ^{13}C and ^{15}N 90° pulse lengths were ~ 1.3 μs and ~ 2.65 μs , respectively. Spectral datasets were processed with 50-200 Hz of line broadening; chemical shifts were referenced externally to the methylene ($-\text{CH}_2-$) group of adamantane (Sigma) at $\delta_{\text{C}}=38.48$ ppm³⁸ or calculated from ^{15}N and ^{13}C gyromagnetic ratios by IUPAC-specified procedures.³⁹

For 1D ^{13}C CPMAS NMR using the 3.2-mm Bruker probes, typical 1-2 ms cross polarization times with ~ 20 -50% linearly ramped rf field strengths⁴⁰ for ^1H and a ~ 50 kHz constant rf field for ^{13}C were used to transfer magnetization from ^1H to ^{13}C nuclear spin baths. High-power heteronuclear proton decoupling (80-100 kHz) was achieved using the two-pulse phase modulated (TPPM) composite pulse sequence,⁴¹ and recycle delays of 3 s were inserted between successive acquisitions. For the 1.6-mm Varian probe, high-power heteronuclear ^1H decoupling (175-185 kHz) was achieved using the small phase incremental alternation (SPINAL) pulse sequence⁴² and acquisition was done with a 3 s recycle delay.

1D ^{15}N CPMAS spectra were also recorded with ramped cross polarization, using 1-3 ms cross polarization times, recycle delays of 2-3 s, and 80-100 kHz ^1H decoupling. Typical experimental parameters on the Bruker spectrometer were as follows: ^1H 90° pulse duration, ~ 3 μs ; ^{15}N 90° pulse duration, 4-6 μs ; ^1H - ^{15}N cross polarization time, 1-3 ms; sweep width, 25-50 kHz; acquisition time, 10 ms; data points, 2048; number of transients, 128-10,000 for ^{15}N -enriched pigments. Typical experimental parameters on the Varian spectrometer were as follows: ^1H 90° pulse duration, 2.3 μs ; ^{15}N 90° pulse duration, 2.65 μs ; sweep width, 50 kHz; acquisition time, 50 ms; data points, 2500; number of transients, 1024-4096.

^{15}N - ^{13}C spin correlations were obtained using double CP-based (DCP) measurements^{43,44} with the Bruker 750 MHz spectrometer and HCN probe. The 2D ^{15}N - ^{13}C DCP correlation spectra were collected with a 1-3 ms initial $^1\text{H} \rightarrow ^{15}\text{N}$ CP step and a 3-4 ms $^{15}\text{N} \rightarrow ^{13}\text{C}$ CP step; MAS rates of 15-23 kHz were used in separate experiments. TPPM ^1H decoupling with an rf field strength corresponding to 80-100 kHz was applied during acquisition. For 2D DCP measurements on CN dopamine melanin pigments, typical experimental parameters were as follows: spectral width for ^{13}C , 75 kHz; spectral width for ^{15}N , 25 kHz; number of scans (direct dimension), 1536; number of points (indirect dimension), 32; three identical data sets (each ~ 24 hr) co-added to produce the final DCP spectra. For 2D DCP measurements on synthetic

melanin pigments derived from the [^{13}C , ^{15}N] L-tyrosine precursor, typical experimental parameters were as follows: spectral width for ^{13}C , 75 kHz; spectral width for ^{15}N , 25 kHz; number of scans (direct dimension), 1024; number of points (indirect dimension), 128; two identical data sets (each ~ 22 hr) co-added to produce the final DCP spectra.

^{15}N - ^{13}C correlations were confirmed with Proton Assisted Inensitive Nuclear Cross-Polarization (PAIN-CP) experiments, which reduce dipolar truncation and hence favor the observation of long distance contacts.^{45,46} A Bruker Avance II spectrometer operating at a ^1H frequency of 900 MHz and equipped with a 3.2-mm HXY E-free probe spinning at 20 kHz was used for these measurements. 2D PAIN-CP spectra of the isotopically enriched synthetic melanin pigments were recorded with a spectral width of ~ 103 kHz in the direct dimension (^{13}C) and ~ 45.6 kHz in the indirect dimension (^{15}N); other parameters included 512 transients (direct dimension), 2048 points in the direct dimension (^{13}C), and 64 points in the indirect dimension (^{15}N).

For 2D ^{13}C - ^{15}N spectral data, acquisition times in the indirect dimension were chosen to limit the total experiment times to 1-3 days; additional resolution was not available by acquiring more data points because signal decay was complete and the sweep width exceeded the spectral window with the selected parameters. An exponential apodization function with 200-400 Hz line broadening was used for the direct-detected dimension, and an exponential apodization function with 100-200 Hz line broadening was applied for the indirect dimension. Identical 1D spectra were observed before and after lengthy 2D NMR experiments, verifying the melanin sample stability.

Results and Discussion

^{13}C and ^{15}N NMR Comparisons of Synthetic and Fungal Melanins

Shown in **Figure 1** are the first ^{13}C and ^{15}N CPMAS NMR spectra reported for melanin pigments derived from [^{13}C , ^{15}N] L-tyrosine by cell-free enzyme-catalyzed polymerization. Comparable 150 MHz one-dimensional (1D) ^{13}C spectra (**Figure S1**) and the expected EPR activity²⁰ are obtained whether this pigment is made from L-tyrosine or L-dopa, supporting previously reported tyrosinase-mediated oxidation from L-tyrosine to L-dopa during the polymerization process.⁷ Both synthetic pigments display aromatic regions (110-160 ppm) similar to CN melanins derived from the obligatory exogenous L-dopa precursor,²⁰⁻²² providing preliminary indications of a common heterogeneous amorphous aromatic core structure in the (natural-abundance) synthetic and fungal melanin pigments. ^{13}C

ARTICLE

NMR spectra for the isotopically enriched materials are dominated by partially resolved arene (and/or alkene) resonances consistent with proposed indole-based aromatic ring structures,^{12,24,26} but additional spectral features are evident from carboxyl groups (168-174 ppm) and open-chain aliphatics (30-60 ppm) as reported for solid fungal melanins^{20-23,27} and the polydopamines discussed below.³⁰ When compared with the L-tyrosine or natural abundance L-dopa starting materials, these polymerized products show 1D ¹³C NMR spectra with broad features attributable to superposition of chemically and magnetically similar structural units and also to the presence of stable free radicals.^{47,48}

hypothesis of a common indole-based aromatic core in melanins formed by fungal biosynthesis or derived from cell-free synthesis using alternative L-tyrosine or L-dopa precursors: a common or similar aromatic framework develops by autopolymerization and when the reaction is mediated by tyrosinase or laccase. The observed ¹⁵N chemical shifts (**Figures 1 and S1**) are also in accord with reports for melanin from *Sepia officinalis* and human hair,²⁸ polydopamines,³⁰ and tryptophan derivatives.⁴⁹ However, the prominent aliphatic amine resonances reported previously in other pigment samples^{24,27,30} are absent from our ¹⁵N L-tyrosine melanin spectra, suggesting that the open-chain aliphatic ¹³C NMR features exhibited by our melanins do not arise from uncyclized amino acid or catecholamine products.

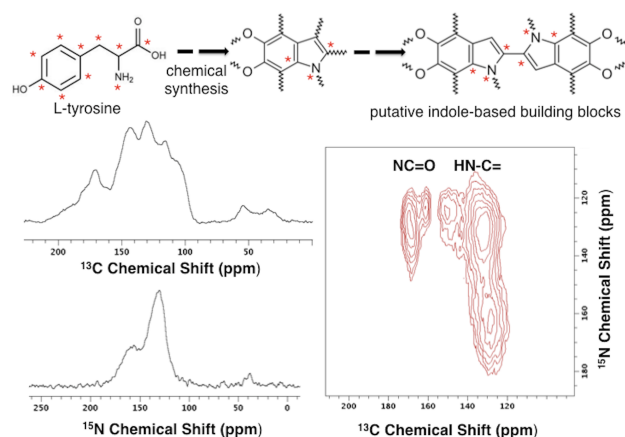


Figure 1. Left: One-dimensional solid-state CPMAS ¹³C (top) and ¹⁵N (bottom) NMR spectra of synthetic [U-¹³C,¹⁵N]-L-tyrosine melanin obtained at a ¹H operating frequency of 750 MHz and spinning rate of 23 kHz. Provisional ¹³C resonance assignments appear in the Results section. Right: Two-dimensional ¹³C-¹⁵N double cross polarization (DCP) NMR⁴³ contour diagram of synthetic [U-¹³C,¹⁵N]-L-tyrosine melanin, obtained with a spinning speed of 23 kHz. The cell-free reactions, for which the isotopic labeling scheme and a possible indole-based structural unit are illustrated, were catalyzed by tyrosinase.

The 75 MHz ¹⁵N NMR spectrum of isotopically enriched L-tyrosine melanin shown in Figure 1 offers the highest resolution view to date of the nitrogen-based pigment architecture, surpassing natural-abundance spectra of synthetic L-dopa melanins and natural pigments from fungal sources.^{24,27} In conformance with these prior reports, our synthetic L-tyrosine melanin displays aromatic resonances at ~130 and ~157 ppm, consistent with a pyrrole within an indole unit and a free pyrrole structure, respectively.³⁰ These results strengthen our ¹³C-based

Two-Dimensional NMR to Delineate Pairwise ¹³C-¹⁵N Proximities in Synthetic and Fungal Melanins

Both the resolution and structural information content of the 1D spectra are improved substantially by the two-dimensional (2D) NMR contour plot of Figure 1, which discriminates among the carbonaceous functional groups by their chemical shifts and reveals which ¹³C nuclei are located within ~4.5-5 Å of particular ¹⁵N partners. Thus, rather than using a collection of observed ¹³C and ¹⁵N chemical shifts to deduce plausible building blocks, double cross polarization⁴³ (DCP) experiments on [U-¹³C,¹⁵N]-L-tyrosine melanin provide direct spectroscopic verification of nearby dipolar-coupled ¹³C-¹⁵N pairs present in the pigment structure. These results, which are confirmed by Proton Assisted Insensitive Nuclei Cross Polarization (PAIN-CP)⁴⁵ methods (**Figure S2**), constitute the first direct assessment of nitrogen-containing molecular architecture in a melanin pigment. Such powerful heteronuclear correlation strategies have been used only rarely in non-crystalline solids,⁵⁰ which typically display compromised cross polarization efficiency and limited spectral resolution.

For eumelanin derived from L-tyrosine, the overlapped 1D ¹³C NMR aromatic core spectral pattern (110-160 ppm) is augmented by a 2D contour plot that reveals five ¹³C-¹⁵N spatially proximal spin pairs, including four chemically distinguishable carbons and three nitrogens. The nearby ¹³C-¹⁵N pairs correspond to cross-peaks at (130, 163), (130, 132), (152, 125), (163, 125), and (168, 132) ppm, indicating the covalent and associative architectural possibilities for intact melanin biopolymer assemblies. For instance, the carboxyl carbon (168 ppm) and several types of

ARTICLE

arene carbons (130, 152, and 163 ppm) are each close in space to one of the two types of indole nitrogens that appear in the ^{15}N spectrum at 125 and 132 ppm, respectively, providing direct support for aromatic building blocks similar to and/or developed from DHICA as well as DHI structural units in the fully formed melanin structure.^{7,9} Conversely, only the arene carbons at ~130 ppm are proximal to the 163-ppm pyrrole nitrogens, consistent with oxidative cleavage of the DHI-based aromatic units that predominate in synthetic melanins⁷ and polydopamines.³⁰ Although the observed pairwise ^{13}C - ^{15}N interactions could also result from oligomer stacking with interlayer distances of 3.1-3.4 Å deduced from DFT calculations,¹⁶ we expected the numerous shorter indole covalent bonds to dominate the observed DCP spectral connectivities. Given the concordance of 1D ^{13}C CPMAS spectra for synthetic L-tyrosine melanin and CN L-dopa melanin, similar structural constraints are expected to characterize the fungal pigment.

1D and 2D NMR for Structures of Synthetic and Fungal Polydopamine Melanins

Finally, the potential of solid-state NMR for investigations of melanin molecular architecture is aptly illustrated for a series of EPR-active pigments derived from a dopamine precursor by laccase-mediated catalysis in the CN fungal cells. **Figures 2 and S3** illustrate the similarity of 1D ^{15}N CPMAS NMR signatures for synthetic and CN [^{13}C , ^{15}N]-dopamine melanins, again supporting a common aromatic core and reinforced by 1D ^{13}C CPMAS spectra with similar aromatic features (but distinctive aliphatic resonances in the 0-50 ppm region)^{5,51} (**Figure S3**). In addition to the major resonances at ~130 and ~157 ppm observed for other melanins,^{24,27,28} the ^{15}N NMR spectra of our dopamine pigments confirm a modest 30-ppm peak assigned previously to amines.³⁰ The similarity of aromatic core structures in fungal and synthetic pigments is underscored by comparison with the 2D DCP spectrum of [^{13}C , ^{15}N]-dopamine CN melanin shown in Figure 2, which replicates the cross-peak pattern and major pairwise nuclear spin proximities of the synthetic [^{13}C , ^{15}N]-tyrosine pigment (Figure 1). No nearby ^{13}C - ^{15}N pairs involving the [^{13}C]-glucose taken up by the cellular medium are evident in the current DCP spectrum. Thus, though this latter 2D NMR result extends the finding of common indole-based core architectures from L-tyrosine and natural-abundance L-dopa precursors to the dopamine neurotransmitter, distinctive spectral features consistent with uncyclized amine-terminated sidechains³⁰ are also revealed for polydopamine.

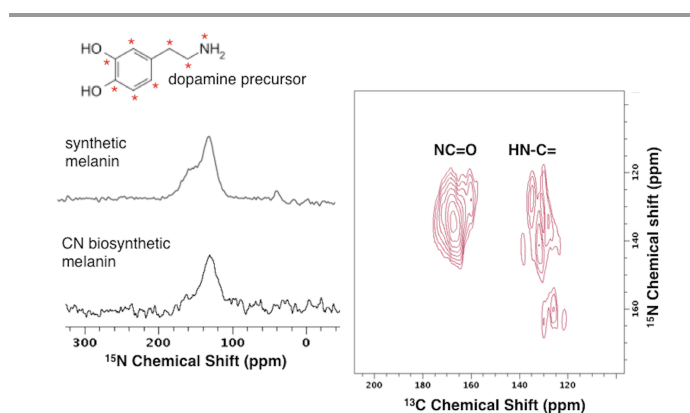


Figure 2. **Left:** One-dimensional solid-state CPMAS ^{15}N NMR spectra of [^{13}C , ^{15}N]-dopamine synthetic and CN melanins obtained at ^1H operating frequencies of 600 MHz and 750 MHz, respectively, and a spinning rate of 15 kHz. **Right:** Two-dimensional ^{13}C - ^{15}N double cross polarization (DCP) NMR⁴³ contour diagram of [^{13}C , ^{15}N]-dopamine CN melanin produced in [^{13}C]-glucose media, obtained at a ^1H operating frequency of 750 MHz with a spinning speed of 10 kHz. The cell-free reaction was catalyzed by tyrosinase in the presence of catalase.

Conclusions

Our ^{13}C and ^{15}N solid-state NMR results demonstrate for the first time that cell-free polymerization of L-tyrosine or L-dopa produces melanins with a common indole-based aromatic core structure in the intact melanin pigments. The indole-related spectral signature is also evident for intact synthetic dopamine and natural-abundance L-dopa CN melanins, thus supporting the development of a similar aromatic pigment core from these three precursors – regardless of whether tyrosinase or laccase catalysts are used and whether the reactions are mediated by fungal cells. Whereas these NMR studies indicate the suitability of the synthetic models for aromatic structural units of the natural pigments, they also reveal distinctive aliphatic moieties depending on how the pigments are formed.

Each reaction pathway produces a heterogeneous, amorphous pigment, and the CN melanins can also bind to cell-wall components.^{20,22} The ^{13}C - ^{15}N dipolar interaction patterns are strikingly similar for the synthetic L-tyrosine melanins and CN dopamine pigments. Both DCP and PAIN-CP NMR spectra of the intact pigments (Figures 1 and S2) implicate structural moieties consistent with previously reported DHICA and DHI

ARTICLE

degradation products.^{7,9,11} Additional open-chain aliphatic carbons that could arise from unreacted L-dopa are evident in both synthetic and CN melanins; aliphatic amine structural elements proposed to arise from coupling of dopamine and/or quinone structural units³⁰ are found uniquely in the dopamine melanins. Our observation of four distinct indole-like/indole-based ¹³C-¹⁵N pairs supports multiple modes of polymeric assembly for this pigment class. In the context of prior computational and experimental evidence arguing in favor of stacked oligomers,^{13,14} the distinct proximal pairwise interactions revealed by our 2D NMR measurements independently demonstrate spatial connectivities that likely result from multiple polymerization pathways contributing to the formation of amorphous, heterogeneous natural and synthetic eumelanins. These atomic-level structural comparisons of intact melanins produced from well-defined precursors set the stage for controlling the development of natural protective pigments and engineering biomaterials for human therapeutics, photoprotection, and environmental remediation.

Acknowledgements

This research was supported by a grant from the U.S. National Institutes of Health (NIH R01-AI052733). The 600 MHz NMR facilities used in this work are operated by The City College and the CUNY Institute for Macromolecular Assemblies, with additional infrastructural support provided by NIH 2G12 RR03060 from the National Center for Research Resources and 8G12 MD007603 from the National Institute on Minority Health and Health Disparities of the National Institutes of Health. R.E.S. is a member of the New York Structural Biology Center (NYSBC). The 750 MHz NMR experiments conducted at the NYSBC are made possible by a grant from the New York State Office of Science, Technology, and Academic Research.

Notes and references

^a Department of Chemistry, City College of New York, Graduate Center and Institute for Macromolecular Assemblies, City University of New York, Department of Chemistry MR-1208B, 160 Convent Avenue, New York, NY 10031-9101, USA

^b Department of Microbiology and Immunology, Albert Einstein College of Medicine, Yeshiva University, Bronx, New York 10461, USA

^c New York Structural Biology Center, New York, NY 10027, USA

Corresponding Authors

rstark@ccny.cuny.edu, schatterjee@ccny.cuny.edu

The authors declare no competing financial interest.

Authors' contributions

S.C. and B.I. designed, conducted, and analyzed the NMR experiments; R.P.R. prepared the fungal melanins; S.T. and S.C. prepared the synthetic melanins; all authors discussed the results and contributed to manuscript preparation; A.C., R.E.S., and S.C. exercised project oversight and wrote the manuscript.

Electronic Supplementary Information (ESI) available: Solid-state NMR spectra including 1D CPMAS ¹³C NMR of melanins from L-tyrosine and L-dopa, 2D ¹³C-¹⁵N PAIN-CP NMR of synthetic [^U-¹³C, ¹⁵N]-L-tyrosine melanin, and CPMAS ¹³C NMR spectra of synthetic and CN dopamine melanins. See DOI: 10.1039/b000000x/

1. H. C. Eisenman and A. Casadevall, *Appl. Microbiol. Biotechnol.*, 2012, **93**, 931–940.
2. P. Meredith, C. J. Bettinger, M. Irimia-Vladu, A. B. Mostert, and P. E. Schwenn, *Rep. Prog. Phys.*, 2013, **76**, 034501.
3. L. Panzella, G. Gentile, G. D'Errico, N. F. Della Vecchia, M. E. Errico, A. Napolitano, C. Carfagna, and M. D'Ischia, *Angew. Chem. Int. Ed.*, 2013, **52**, 12684–12687.
4. J. D. Simon and D. N. Peles, *Accs. Chem. Res.*, 2010, **43**, 1452–1460.
5. K.-Y. Ju, Y. Lee, S. Lee, S. B. Park, and J.-K. Lee, *Biomacromolecules*, 2011, **12**, 625–632.
6. E. Buszman, B. Pilawa, and T. Witoszy, *Appl. Magn. Reson.*, 2003, **24**, 401–407.
7. S. Ito, *Pig. Cell. Res.*, 2003, **16**, 230–236.
8. M. E. Lyng, R. van der Westen, A. Postma, and B. Städler, *Nanoscale*, 2011, **3**, 4916–4928.

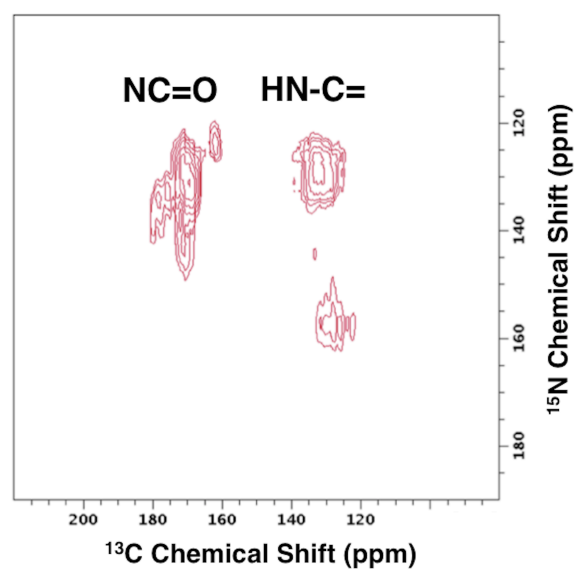
ARTICLE

9. M. d'Ischia, A. Napolitano, A. Pezzella, P. Meredith, and T. Sarna, *Angew. Chem. Int. Ed.*, 2009, **48**, 3914–3921.
10. O. Crescenzi, C. Kroesche, W. Hoffbauer, M. Jansen, A. Napolitano, G. Prota, and M. G. Peter, *Liebigs Ann. Chem.*, 1994, 563–567.
11. M. d'Ischia, K. Wakamatsu, A. Napolitano, S. Briganti, J.-C. Garcia-Borron, D. Kovacs, P. Meredith, A. Pezzella, M. Picardo, T. Sarna, J. D. Simon, and S. Ito, *Pig. Cell Melan. Res.*, 2013, **26**, 616–633.
12. G. Prota, *Melanins and Melanogenesis*, Academic Press, San Diego, 1992.
13. G. Zajac, J. Gallas, J. Cheng, M. Eisner, S. Moss, and A. Alvarado-Swaisgood, *Biochim. Biophys. Acta*, 1994, **1199**, 271–278.
14. J. Cheng, S. Moss, and M. Eisner, *Pig. Cell. Res.*, 1994, **7**, 255–262.
15. P. Meredith and T. Sarna, *Pig. Cell. Res.*, 2006, **19**, 572–594.
16. S. Meng and E. Kaxiras, *Biophys. J.*, 2008, **94**, 2095–2105.
17. J. D. Simon, D. Peles, K. Wakamatsu, and S. Ito, *Pig. Cell Melan. Res.*, 2009, **22**, 563–579.
18. P. R. Williamson, *J. Bacteriol.*, 1994, **176**, 656–664.
19. P. R. Williamson, K. Wakamatsu, and S. Ito, *J. Bacteriol.*, 1998, **180**, 1570–1572.
20. S. Chatterjee, R. Prados-Rosales, S. Frases, B. Itin, A. Casadevall, and R. E. Stark, *Biochemistry*, 2012, **51**, 6080–6088.
21. S. Tian, J. Garcia-Rivera, B. Yan, A. Casadevall, and R. E. Stark, *Biochemistry*, 2003, **42**, 8105–8109.
22. J. Zhong, S. Frases, H. Wang, A. Casadevall, and R. E. Stark, *Biochemistry*, 2008, **47**, 4701–4710.
23. M. Schnitzer and Y. K. Chan, *Soil Sci. Soc. Am. J.*, 1986, **50**, 67–71.
24. G. A. Duff, J. E. Roberts, and N. Foster, *Biochemistry*, 1988, **27**, 7112–7116.
25. M. G. Peter and H. Forster, *Angew. Chem. Int. Ed.*, 1989, **28**, 741–743.
26. M. Herve, J. Hirschinger, P. Granger, P. Gilard, A. Deflandre, and N. Goetz, *Biochim. Biophys. Acta*, 1994, **1204**, 19–27.
27. H. Knicker, G. Almendros, F. J. Gonzalez-Vila, H. D. Luedemann, and F. Martin, *Org. Geochem.*, 1995, **23**, 1023–1028.
28. B. B. Adhyaru, N. G. Akhmedov, A. R. Katritzky, and C. R. Bowers, *Magn. Res. Chem.*, 2003, **41**, 466–474.
29. P. Thureau, F. Ziarelli, A. Thévand, R. W. Martin, P. J. Farmer, S. Viel, and G. Mollica, *Chem. Eur. J.*, 2012, **18**, 10689–10700.
30. N. F. Della Vecchia, R. Avolio, M. Alfè, M. E. Errico, A. Napolitano, and M. d'Ischia, *Adv. Funct. Mater.*, 2013, **23**, 1331–1340.
31. S. Aime, M. Fasano, B. Bergamasco, L. Lopiano, and G. Quattrocchio, *Adv. Neurol.*, 1996, **69**, 263–270.
32. M. Jastrzebska, A. Kocot, and L. Tajber, *J. Photochem. Photobiol. B*, 2002, **66**, 201–206.
33. S. Ghiani, S. Baroni, D. Burgio, G. Digilio, M. Fukuhara, P. Martino, K. Monda, C. Nervi, A. Kiyomine, and S. Aime, *Magn. Reson. Chem.*, 2008, **46**, 471–479.
34. J. Garcia-Rivera, H. C. Eisenman, J. D. Nosanchuk, P. Aisen, O. Zaragoza, T. Moadel, E. Dadachova, and A. Casadevall, *Fung. Gen. Biol.*, 2005, **42**, 989–998.
35. Á. L. Rosas, J. D. Nosanchuk, M. Feldmesser, G. M. Cox, H. C. McDade, A. Casadevall, N. L. Rosas, H. C. McDade, and A. Casadevall, *Infect. Immun.*, 2000, **68**, 2845–2853.
36. Y. Wang, P. Aisen, and A. Casadevall, *Infect. Immun.*, 1996, **64**, 2420–2424.
37. J. Folch, M. Lees, and G. Stanley, *J. Biol. Chem.*, 1957, **226**, 497–509.
38. C. R. Morcombe and K. W. Zilm, *J. Magn. Res.*, 2003, **162**, 479–486.
39. R. K. Harris, E. D. Becker, S. M. C. D. E. Menezes, R. Goodfellow, and P. Granger, *Pure Appl. Chem.*, 2001, **73**, 1795–1818.
40. G. Metz, X. Wu, and S. O. Smith, *J. Magn. Reson. A*, 1994, **110**, 219–227.

ARTICLE

41. A. E. Bennett, C. M. Rienstra, M. Auger, K. V Lakshmi, and R. G. Griffin, *J. Chem. Phys.*, 1995, **103**, 6951–6958.
42. B. M. Fung, A. K. Khitrin, and K. Ermolaev, *J. Magn. Res.*, 2000, **142**, 97–101.
43. J. Schaefer, R. A. McKay, and E. O. Stejskal, *J. Magn. Res.*, 1979, **34**, 443–447.
44. J. Schaefer, E. O. Stejskal, J. R. Garbow, and R. A. McKay, *J. Magn. Res.*, 1984, **59**, 150–156.
45. J. R. Lewandowski, G. De Paëpe, and R. G. Griffin, *J. Am. Chem. Soc.*, 2007, **129**, 728–729.
46. G. De Paëpe, J. R. Lewandowski, A. Loquet, M. Eddy, S. Megy, A. Böckmann, and R. G. Griffin, *J. Chem. Phys.*, 2011, **134**, 095101.
47. C. C. Felix, J. S. Hyde, T. Sarna, and R. C. Sealy, *J. Am. Chem. Soc.*, 1978, **100**, 3922–3926.
48. R. Sealy, J. Hyde, C. Felix, I. Menon, and G. Prota, *Science (80-)*, 1982, **217**, 545–547.
49. A. T. Petkova, M. Hatanaka, C. P. Jaroniec, J. G. Hu, M. Belenky, M. Verhoeven, J. Lugtenburg, R. G. Griffin, and J. Herzfeld, *Biochemistry*, 2002, **41**, 2429–2437.
50. J. R. Lewandowski, P. C. van der Wel, M. Rigney, N. Grigorieff, and R. G. Griffin, *J. Am. Chem. Soc.*, 2011, **133**, 14686–14698.
51. D. R. Dreyer, D. J. Miller, B. D. Freeman, D. R. Paul, and C. W. Bielawski, *Langmuir*, 2012, **28**, 6428–6435.

ARTICLE

Table of Contents (TOC) Graphic

TEXT: Comparing natural and synthetic eumelanin pigment structures: High-field two-dimensional solid-state nuclear magnetic resonance reveals a common indole-based aromatic core for ubiquitous protective pigments that inspire engineered materials.